1521-0111/12/8202-189–198$25.00
MOLECULAR PHARMACOLOGY
Vol. 82, No. 2
77271/3781394

Mol Pharmacol 82:189–198, 2012

DC120, a Novel and Potent Inhibitor of AKT Kinase, Induces Tumor Cell Apoptosis and Suppresses Tumor Growth[S]

Rong Deng, Fen Yang, Shao-hua Chang, Jun Tang, Juan Qin, Gong-Kan Feng, Ke Ding, and Xiao-Feng Zhu

State Key Laboratory of Oncology in South China (R.D., F.Y., J.T., J.Q., G.-K.F., X.-F.Z.) and Department of Breast Oncology, Cancer Center, Sun Yat-sen University, Guangzhou, China (J.T.); Key Laboratory of Regenerative Biology and Institute of Chemical Biology, Guangzhou Institutes of Biomedicine and Health, Chinese Academy of Sciences, Guangzhou, China (S.C., K.D.); and Graduate School of Chinese Academy of Sciences, Beijing, China (S.C., K.D.)

Received December 18, 2011; accepted April 26, 2012

ABSTRACT

Protein kinase B/AKT kinase is the core component of the phosphatidylinositol 3-kinase/AKT signaling pathway, which is frequently hyperactivated in human cancers. We designed and synthesized a series of 2-pyrimidyl-5-amidothiazole compounds based on the ATP binding site of AKT, and the most potent compound, (*S*)-*N*-(1-amino-3-(2,4-dichlorophenyl)propan-2-yl)-2-(2-(methylamino)pyrimidin-4-yl)thiazole-5-carboxamide (DC120), was identified to inhibit AKT activity in vitro with an EC_{50} of 153 nM by a fluorescence resonance energy transfer-based Z′-LYTE assay. The antitumor effect of DC120 was tested on human CNE2 and MDA-MB-453 cell lines and the CNE2 xenograft model. The results showed that DC120 could obviously inhibit the proliferation of CNE2 and MDA-MB-453 cells via induction of apoptosis, with the evidence of increases in sub-G_1 and annexin V-positive cells, characteristic morphologic changes of apoptosis in the nucleus, and cleaved caspase-3. Further study showed that MDA-MB-453 cells transfected with constitutively activated AKT1 were more sensitive to DC120,whereas CNE2 cells with knockdown of AKT1 expression by short hairpin RNA were more resistant to DC120. Of more importance, DC120 partially attenuated the phosphorylation levels of forkhead transcription factor (FKHR), FKHRL1, glycogen synthase kinase 3β, and mammalian target of rapamycin in a dose-dependent and time-dependent fashion and led to an increase in the nuclear accumulation of exogenous FKHR in cancer cells. In addition, DC120 at 20 mg/kg/day inhibited the CNE2 xenograft tumor growth with a treated group/control group ratio of 38.1%, accompanied by increasing terminal deoxynucleotidyl transferasedUTP nick-end labeling-positive cells in the tumor sample. In addition, DC120 induced a feedback loop to activate the mitogen-activated protein kinase pathway and treatment with mitogen-activated protein kinase kinase inhibitor 1,4-diamino-2,3-dicyano-1,4-bis(methylthio)butadiene (U0126) and DC120 synergistically induced cancer cell apoptosis. These data provide validation for the development of DC120 to treat cancers displaying elevated levels of AKT.

Introduction

Protein kinase B/AKT kinase, a serine/threonine kinase, is the core component of the phosphoinositide 3-kinase/AKT signaling pathway and therefore is involved in a wide variety of biological processes, including cell proliferation, differentiation, apoptosis, autophagy, glucose metabolism, the repair of DNA double-strand breaks, and tumorigenesis (Bellacosa et al., 2005; Manning and Cantley, 2007; Tokunaga et al., 2008; Deng et al., 2011; Janku et al., 2011). It is well estab-

This work was supported by the Nature Science Foundation of China [Grant 81001446]; Major science and technology project of the National Basic Research Program (973 Program) of China (2012CB967004); Nature Science Foundation of Guangdong province [Grant 10451008901004533]; Medical Scientific Research Foundation of Guangdong province [Grant B2010109]; and Foundation for Distinguished Young Scholars of Sun Yat-Sen University [Grant10ykpy39].

R.D., F.Y., and S.C. contributed equally to this work.

Article, publication date, and citation information can be found at http://molpharm.aspetjournals.org.
http://dx.doi.org/10.1124/mol.111.077271.

[S] The online version of this article (available at http://molpharm.aspetjournals.org) contains supplemental material.

ABBREVIATIONS: MK-2206,8-[4-(1-aminocyclobutyl)phenyl]-9-phenyl-1,2,4-triazolo[3,4-*f*][1,6]naphthyridin-3(2*H*)-one dihydrochloride; GDC0068, (*S*)-2-(4-chlorophenyl)-1-(4-((5*R*,7*R*)-7-hydroxy-5-methyl-6,7-dihydro-5*H*-cyclopenta[d]pyrimidin-4-yl)piperazin-1-yl)-3-(isopropylamino)propan-1-one; DC120, (*S*)-*N*-(1-amino-3-(2,4-dichlorophenyl)propan-2-yl)-2-(2-(methylamino)pyrimidin-4-yl)thiazole-5-carboxamide; MAPK, mitogen-activated protein kinase; MEK, mitogen-activated protein kinase kinase; U0126, 1,4-diamino-2,3-dicyano-1,4-bis(methylthio)butadiene; DMSO, dimethyl sulfoxide; GSK, glycogen synthase kinase; FKHR, forkhead transcription factor; mTOR, mammalian target of rapamycin; DAPI, 4,6-diamidine-2-phenylindole; MTT, 3-[4,5-dimethylthiazol-2 -thiazolyl]-2,5-diphenyltetrazolium bromide; PI, propidium iodide; shRNA, short hairpin RNA; CTX cyclophosphamide; TUNEL, terminal deoxynucleotidyl transferase dUTP nick-end labeling; JNK, c-Jun NH_2-terminal kinase; ERK, extracellular signal-regulated kinase; A-443654, (*S*)-1-(1*H*-indol-3-ylmethyl)-2-[5-(3-methyl-1*H*-indazol-5-yl)-pyridin-3-yloxy]-ethylamine;GSK690693, 4-[2-(4-amino-1,2,5-oxadiazol-3-yl)-1-ethyl-7-[(3*S*)-3-piperidinylmethoxy]-1*H*-imidazo[4,5-*c*]pyridin-4-yl]-2-methyl-3-butyn-2-ol.

lished that hyperactivation of AKT kinase is a common event in many human cancers, and elevated AKT activity can also be detected in preneoplastic lesions (Balsara et al., 2004; Bellacosa et al., 2005; Caporali et al., 2008). Loss or mutation of tumor suppressor phosphatase and tensin homolog, amplification or mutation of phosphoinositide 3-kinase, activation or mutation of growth factor receptors and oncogenes, and amplification of AKT itself are involved in activation of AKT in tumors (Tokunaga et al., 2008; Kalinsky et al., 2011; Whitehall et al., 2011). Activation of AKT promotes the development or progression of cancer as well as resistance to treatment with chemotherapy and/or radiation therapy. In addition, immunohistochemical analyses have shown that AKT activation is a poor prognostic factor in various cancers (LoPiccolo et al., 2007; Nakanishi and Ross, 2012; Wei and Xu, 2011). Therefore, AKT is an attractive target for cancer therapy, and it has been proven that inhibition of AKT alone or in combination with conventional chemotherapeutic agents or radiotherapy can reduce the apoptotic threshold and preferentially kill cancer cells (Crowell et al., 2007; Engelman, 2009; Liu et al., 2012; Sun et al., 2011).

AKT kinase has been an attractive target for small molecular drug discovery. To date, researchers have developed many AKT inhibitors, including inhibitors targeting the ATP-binding site, pleckstrin homology domain, or protein substrate binding site of AKT. Several of them, such as 8-[4-(1-aminocyclobutyl)phenyl]-9-phenyl-1,2,4-triazolo[3,4-*f*][1,6]naphthyridin-3(2*H*)-one dihydrochloride (MK-2206), (*S*)-2-(4-chlorophenyl)-1-(4-((5*R*,7*R*)-7-hydroxy-5-methyl-6,7-dihydro-5*H*-cyclopenta[d]pyrimidin-4-yl)piperazin-1-yl)-3-(isopropylamino)propan-1-one (GDC0068), and perifosine are currently in phase I to II trials alone or in combination to treat multiple forms of cancer (Hers et al., 2011; Richardson et al., 2011). In the present study, we analyzed the crystal structures of the published ATP-competitive AKT inhibitors bound to AKT kinases (Lin et al., 2006; Zhu et al., 2007; Seefeld et al., 2009; McHardy et al., 2010) and optimized the screened hit compounds to a series of 2-(methylaminopyrimidinyl) thiazole-5-carboxamide derivatives (Chang et al., 2012). We screened out (*S*)-*N*-(1-amino-3-(2,4-dichlorophenyl)propan-2-yl)-2-(2-(methylamino)pyrimidin-4-yl)thiazole-5-carboxamide (DC120) from these compounds by a fluorescence resonance energy transfer-based Z′-LYTE assay (EC_{50} = 153 nM) and focused on the antitumor activity of this potent compound. Our data showed that DC120 exhibited an inhibitory effect on proliferation in human nasopharyngeal carcinoma CNE2 cells and human breast cancer MDA-MB-453 cells via inducing cell apoptosis and significantly reduced tumor growth of CNE2 xenografts. In addition, we observed that inhibition of AKT kinase activity and blockade of the AKT downstream signaling pathway in cancer cells were involved in antitumor activity of DC120. Moreover, we found that DC120 induced a feedback loop to activate the MAPK pathway and the combination of the MEK inhibitor 1,4-diamino-2,3-dicyano-1,4-bis(methylthio)butadiene (U0126) and DC120 has a significant synergistic effect.

Materials and Methods

DC120 Preparation. For all in vitro studies, compound DC120 (structure shown in Fig. 2A) was dissolved in DMSO at a concentration of 50 mM and stored at −20°C. For the tumor xenograft studies, DC120 was formulated in 8% solvent diluent [(DMSO/(Cremophor EL + ethanol), 1:3] at a concentration of 50 mg/ml.

Cell Culture and Reagents. Human nasopharyngeal carcinoma CNE2 and human breast cancer MDA-MB-453 cells were cultivated in DMEM supplemented with 10% fetal bovine serum in a 5% CO_2 humidified atmosphere at 37°C. Glyceraldehyde-3-phosphate dehydrogenase, AKT, phospho-AKT (Ser473), phospho-AKT (Thr308), GSK3α/β, caspase-3, and horseradish peroxidase-conjugated second antibodies were purchased from Santa Cruz Biotechnology, Inc. (Santa Cruz, CA). Anti-phospho-FKHR, phospho-FKHRL1, phospho-GSK3β, phospho-mTOR, cleaved caspase-3, mTOR, and chemiluminescence reagents were obtained from Cell Signaling Technology (Danvers, MA). Anti-Flag antibody, DAPI, MTT, and DMSO were purchased from Sigma (St. Louis, MO, USA).

Z′-LYTE Kinase Assay. A fluorescence resonance energy transfer-based Z′-LYTE kinase assay kit−Ser/Thr 6 peptide (Invitrogen, Carlsbad, CA) was used to evaluate the EC_{50} value of these 2-pyrimidyl-5-amidothiazole compounds for inhibition of AKT1 kinase. The reaction was performed on a 384-well plate with a 10-μl reaction volume per well containing 2 μM Ser/Thr 6 peptide substrate in 50 mM HEPES, pH 7.5, 0.01% Brij-35, 10 mM $MgCl_2$, 1 mM EGTA, and an appropriate amount of AKT1 kinase with a serial 3-fold dilution of test compound. The final reaction concentration of ATP was 75 μM. After a 1-h incubation, a reaction was developed and terminated, and the fluorescence ratio was calculated according to the manufacturer's protocol. Staurosporine was used as a positive control. A dose-response curve was fitted using Prism 5.0 (GraphPad Software Inc., San Diego, CA).

MTT Assay. Cells were seeded on a 96-well plate (Falcon; BD Biosciences Discovery Labware, Bedford, MA) at 5000 to 8000 cell density per well, and different concentrations of compounds were added to the medium and incubated for an indicated period. Cell viability was determined by the MTT assay as described previously (Deng et al., 2009). The IC_{50} value was calculated with CalcuSyn software (Biosoft, Cambridge, UK).

Annexin V-Fluorescein Isothiocyanate Apoptosis Assay. An annexin V-FLUOS Staining Kit (Roche, Basel, Switzerland) was used to evaluate DC120-induced apoptosis. Cells were cultured on a six-well plate and exposed to DC120. The cells were harvested and stained with annexin V-FLUOS solution and PI solution provided with the kit for 10 to 15 min. Apoptosis was immediately analyzed with a flow cytometer (Beckman Coulter, Fullerton, CA) at the wavelength of 488 nm.

DAPI Nuclear Staining Assay. For detecting DC120-induced apoptosis, cells were subcultured on a 24-well plate covered with 13 mm × 13 mm slips and exposed to DC120. The cells were fixed with 10% absolute methanol permeabilized by 0.25% Triton X-100 and stained with DAPI (1 μg/ml) for 10 min. The morphologic changes of apoptosis-characteristic nuclei were examined with a confocal microscope (Olympus, Tokyo, Japan).

Cell Cycle Analysis. For detecting DC120-induced apoptosis, cells were cultured in six-well plates and exposed to DC120. The cells were harvested and fixed with 70% ethanol and incubated overnight at −4°C. Then the cells were washed and resuspended in 1 ml of staining solution (50 μg/ml PI and 50 μg/ml RNase) for 15 min. The PI fluorescence associated with DNA was measured with a flow cytometer. The percentages of nuclei in the sub-G_1 phase of the cell cycle were calculated by MultiCycle software.

Western Blot Analysis. The cells were harvested and lysed in 1× cell lysis buffer (Cell Signaling Technology) with addition of 1 mM phenylmethanesulfonyl fluoride immediately before use. The protein concentration was estimated with a Pierce BCA protein assay kit. Equal amounts of protein (20–40 μg) were separated electrophoretically on 8 to 15% SDS-polyacrylamide gels and transferred onto polyvinylidene difluoride membranes (Millipore Corporation, Billerica, MA) and analyzed as described previously (Deng et al., 2009).

Plasmids and Transfection. For inhibition of AKT activity, the short hairpin RNA (shRNA) sequences against AKT1 (5′-GC-

TACTTCCTCCTCAAGAATG-3′) (Irie et al., 2005) were synthesized by Invitrogen Life Technologies (Shanghai, China) and cloned into the retroviral vector (pSUPER RNAi.puro). The CNE2 cells stably expressing AKT1 shRNA were established by infection with retrovirus-containing supernatants as described previously (Zhou et al., 2009). For activation of AKT activity, MDA-MB-453 cells were transiently transfected with activated myr-AKT1 (Millipore) using Lipofectamine 2000 (Invitrogen, Carlsbad, CA) according to the protocol suggested by the manufacturer. After 24 h of transfection, the cells were used for further experiments.

Immunofluorescence Staining. For detecting the cellular localization of exogenous FKHR, cells were subcultured on a 24-well plate covered with 13 mm × 13 mm slips and transiently transfected with pCDNA3-Flag-FKHR plasmids using Lipofectamine 2000 for 24 h. After DC120 treatment, cells were fixed and permeabilized. Then the cells were incubated with monoclonal anti-Flag antibody (diluted 1:500) for 2 h and Alexa Fluor 488 goat anti-mouse IgG antibody (diluted 1:400) for 1 h. For frozen sections of tumor tissue samples, the cells were incubated with anti-phospho-GSK3β antibody (1:200) at 4°C overnight and Alexa Fluor 488 goat anti-rabbit IgG antibody (1:400) for 1 h. After counterstaining with DAPI, the cells on coverslips or sections of tumor tissue were observed using a confocal microscope (Olympus). For frozen sections of tumor tissue samples, the intensity of immunofluorescence representing the expression of phospho-GSK3β protein was evaluated by repeated staining of the same specimens and by two observers. Grading was as follows: −, for no immunofluorescence; ±, for weak and indefinitely detectable immunofluorescence; +, for weak but definitely detectable immunofluorescence; ++, for moderate immunofluorescence; and +++, for intense immunofluorescence (Zhang et al., 2008; Deng et al., 2009).

In Vivo Antitumor Activity. BALB/c nude mice were obtained from Hunan Slac Jingda Laboratory Animal Co. Ltd (Changsha, China) and were 4 to 6 weeks old. All manipulations were performed under sterile conditions. The procedures involving mice and their care were in accordance with the National Institutes of Health *Guide for the Care and Use of Laboratory Animals* (Institute of Laboratory Animal Resources, 1996) and the United Kingdom Co-ordinating Committee on Cancer Research (1998). Tumor xenografts were established by 2×10^6 CNE2 cells injected subcutaneously into nude mice. Mice were randomly divided into three groups, and each group contained six mice. Treatments were initiated on day 7 after inoculation, by which time the tumor volume had reached ~50 mm^3; for each group, 8% solvent diluent (vehicle, negative control), 100 mg/kg CTX every 5 days (positive control), and DC120 (20 mg/kg/day) were administered intraperitoneally for 21 days. Tumor volumes and body weight of mice were observed. Tumor volumes were calculated by the formula: $0.5 \times a \times b^2$ in millimeters, where a is the length and b is the width. When all control tumors developed to more than 2000 mg, nude mice were sacrificed. After the tumor tissues were excised and weighed, the tissue samples were made into frozen sections with 4-mm-width immediately and fixed in ice-cold acetone. Then the frozen sections were stored at −80°C for future studies. Tumor growth inhibition (T/C percentage), which was used to evaluate the tumor response to the drugs, was calculated using the ratio of the average tumor weight of the treated group (T) to the average tumor weight of the control group (C).

TUNEL Staining Assay. An In Situ Cell Death Detection Kit (Roche) was used to evaluate DC120-induced apoptosis in vivo. Frozen tumor sections were incubated in blocking solution for 10 min and permeabilization solution for 2 min on ice. Then 50 μl of TUNEL reaction mixture was added to samples for 60 min at 37°C in a humidified atmosphere in the dark. After counterstaining with DAPI (1 μg/ml), frozen sections were observed using a confocal microscope. TUNEL-positive nuclei were stained green, and all other nuclei were stained blue (Markaryan et al., 2008).

Statistical Analysis. Student's t test was used to evaluate the statistical significance of the result at the 95% confidence level, and $P < 0.05$ was considered to indicate statistical significance.

Results

DC120 Inhibited AKT Kinase Activity In Vitro. We used a biochemistry method (Z′-LYTE Kinase Assay Kits−Ser/Thr 6 Peptide) to evaluate the effect of these 2-(methylaminopyrimidinyl) thiazole-5-carboxamide compounds on the AKT kinase activity in a cell-free system. In this experiment, Z′-LYTE−Ser/Thr 6 Peptide was used as a substrate; Thus, the changes in Z′-LYTE−Ser/Thr 6 Peptide phosphorylation can directly reflect the AKT kinase activity. As expected, we screened out several compounds including DC120. The results showed that DC120 could concentration dependently suppress phosphorylation of Z′-LYTE−Ser/Thr 6 Peptide with an EC_{50} value of approximately 153 nM, whereas the EC_{50} value for staurosporine (positive control) was approximately 122 nM (Fig. 1). We also used an HTScan Akt1 Kinase Assay Kit to confirm the AKT-inhibitory effect of DC120. The results showed that DC120 could concentration dependently suppress phosphorylation of endothelial nitric-oxide synthase (Ser1177) (Supplemental Table 1). To further test whether DC120 has off-target effects, we also used the in vitro competition binding assay of KINOMEscan to evaluate DC120 against a panel of distinct human protein kinases. The results showed that DC120 selectively inhibited AKT but not JNK, ERK, P38, epidermal growth factor receptor, CDK2, and others. At the concentration of 100 nM DC120, the percentage of AKT kinase binding to the immobilized ligand was only 15% (Supplemental Table 2). Taken together, all these data indicated that DC120 could obviously inhibit AKT kinase activity in vitro.

DC120 Suppressed Proliferation and Induced Apoptosis in Cancer Cells. To investigate the cytotoxicity of DC120 in cancer cells, we performed an MTT assay. DC120 displayed potent cytotoxicity in diversified cancer cell lines including nasopharyngeal carcinoma (CNE1, CNE2, and HONE1), hepatocellular cancer (HepG2, SMMC7721, and Bel-7402), melanoma (SK-MEL-1 and ME-4405), and breast cancer (MDA-MB-453, MDA-MB-436, and MDA-MB-435). The IC_{50} values for all the tumor cell lines tested varied from 5 to 10 μM (Supplemental Fig. 1). In this study, we focused on the effect of DC120 on CNE2 and MDA-MB-453 cell lines, which showed more aberrantly activated AKT signaling pathway than cells observed in our previous work. As shown in Fig. 2, DC120 obviously suppressed cell viability in a dose-dependent manner. At 72 h, the IC_{50} values were 7.09 μM in CNE2 cells and 6.48 μM in MDA-MB-453 cells (Fig. 2B).

To confirm whether the growth inhibition of DC120 was caused by apoptosis in cells, the sub-G_1 fraction and the percentage of annexin V-positive cells were tested using flow cytometric analysis. After cancer cells were treated with different concentrations of DC120, the sub-G_1 fraction and the percentage of annexin V-positive cells markedly increased. When the cells were exposed to 20 μM DC120 for 48 h, the rates of sub-G_1 fraction increased from 0.3% up to 45.9% in CNE2 cells and from 0.9% up to 60.2% in MDA-MB-453 cells (Fig. 3A); With exposure to 20 μM DC120 for 44 h, the percentage of annexin V-positive cells increased from 1.0% up to 47.2% in CNE2 cells and from 1.8% up to 61.1% in MDA-MB-453 cells (Fig. 3B). Moreover, cell morphology with DAPI staining identified the apoptotic cell population. Figure 3C shows that treatment with 0.1% DMSO did not appreciably induce apoptosis in cells, but typical morphological

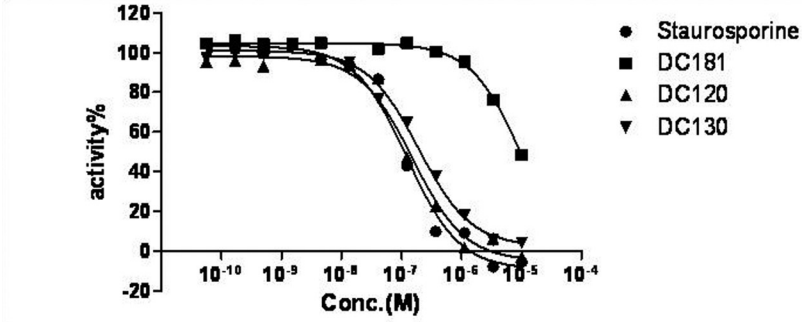

	Staurosporine	DC181	DC120	DC130
LogEC50	-6.911	-4.959	-6.817	-6.718
EC50	1.226e-007	1.099e-005	1.525e-007	1.915e-007

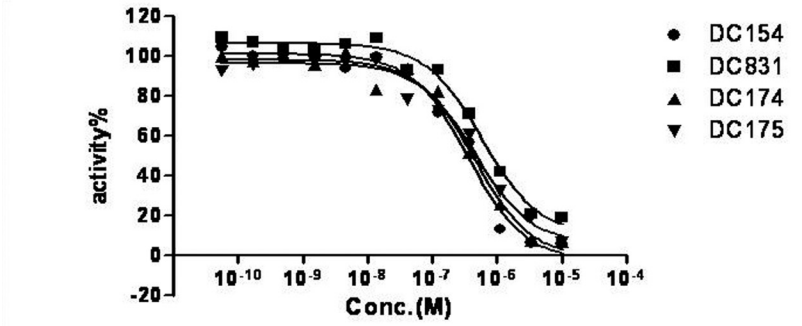

	DC154	DC831	DC174	DC175
LogEC50	-6.449	-6.234	-6.350	-6.346
EC50	3.559e-007	5.838e-007	4.463e-007	4.506e-007

Fig. 1. The effect of 2-(methylaminopyrimidinyl) thiazole-5-carboxamide compounds on the AKT kinase activity in a cell-free system. AKT1 kinase activity was determined using a Ser/Thr 6 peptide substrate, AKT1 kinase, ATP, and different concentrations of compounds in the presence of kinase buffer for 60 min as described under *Materials and Methods* with the Z′-LYTE assay. Staurosporine was used as a positive control. The dose-response curve was fitted using Prism 5.0. DC130, (*S*)-*N*-(1-amino-3-phenylpropan-2-yl)-2-(2-(methylamino)pyrimidin-4-yl) thiazole-5-carboxamide; DC154, (*S*)-*N*-(1-amino-3-(2,4-dichlorophenyl)propan-2-yl)-4-methyl-2-(2-(methylamino)pyrimidin-4-yl)thiazole-5-carboxamide; DC174, (*S*)-*N*-(1-amino-3-(4-chlorophenyl)propan-2-yl)-2-(2-(methylamino)pyrimidin-4-yl)thiazole-5-carboxamide; DC175, (*S*)-*N*-(1-amino-3-(1H-indol-3-yl)propan-2-yl)-2-(2-(methylamino)pyrimidin-4-yl)thiazole-5-carboxamide; DC181, (*S*)-*N*-(1-amino-3-(4-hydroxyphenyl)propan-2-yl)-2-(2-(methylamino) pyrimidin-4-yl)thiazole-5-carboxamide; DC831, (*S*)-*N*-(1-amino-3-p-tolylpropan-2-yl)-2-(2-(methylamino)pyrimidin-4-yl)thiazole-5-carboxamide.

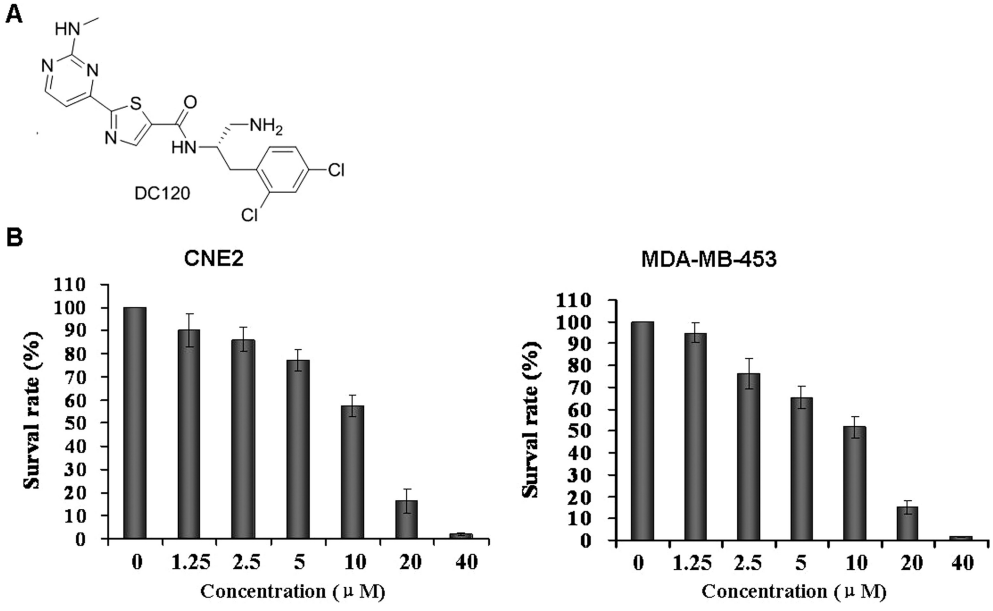

Fig. 2. DC120 inhibited cancer cell proliferation. A, chemical structure of DC120. B, effect of DC120 on proliferation of CNE2 and MDA-MB-453 cells. Cells were cultured in a 96-well plate, exposed to different concentrations of DC120, and incubated for 72 h. Each column represented the mean ± S.D. of triplicate determinations.

changes associated with apoptosis-chromatin condensation, apoptotic body formation, and DNA fragmentation were prevalently observed in DC120-treated CNE2 and MDA-MB-453 cells. Furthermore, procaspase-3 cleaved to yield 17/19-kD fragmentation that was also detected in CNE2 and MDA-MB-453 cells after DC120 treatment (Fig. 3D). These data indicated that DC120 indeed induced apoptosis in cancer cells, which was consistent with the results of the MTT growth inhibition assay.

Growth Inhibition of DC120 on Cancer Cells Depending on AKT Activity. To further confirm DC120 targeting of AKT kinase, retroviral vectors encoding shRNA sequences against AKT1 were stably transfected to CNE2 cells. The down-regulation of phospho-AKT and AKT1 was at least 75% (Fig. 4A, left), and the inhibitory rate in CNE2/AKT1 shRNA cells was obviously lower than that in control cells after treatment with DC120 ($p < 0.01$) (Fig. 4B, left). On the other hand, myr-AKT1 plasmids (constitutively activated

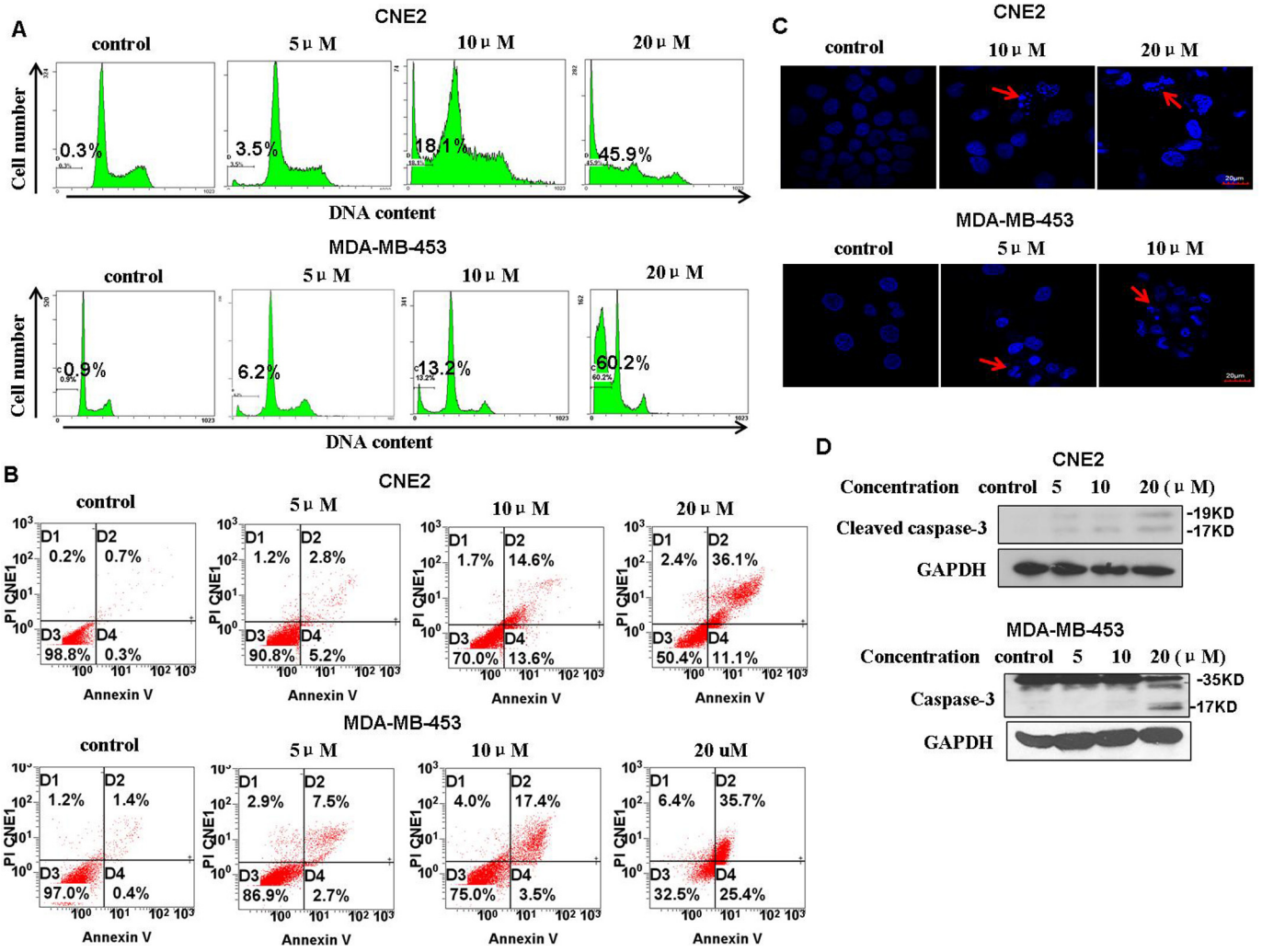

Fig. 3. DC120 induced cancer cell apoptosis. A, CNE2 and MDA-MB-453 cells were treated with different concentrations of DC120 for 48 h, and PI fluorescence associated with DNA was measured by flow cytometry. B, annexin V/PI analysis of CNE2 and MDA-MB-453 cells treated with different concentrations of DC120 for 44 h. DC120 treatment increased the percentages of annexin V^+/PI^- (bottom right quadrant, D4) and annexin V^+/PI^+ (top right quadrant, D2) cells. C, Characteristic apoptosis was seen in CNE2 cells treated with DC120 for 48 h and in MDA-MB-453 cells treated with DC120 for 24 h. Original magnification, 100×. D, treatment of cells with different concentrations of DC120 for 48 h (CNE2 cell line) or 24 h (MDA-MB-453 cell line). Western blot analysis was conducted with cleaved caspase-3 antibody or caspase-3 antibody probes. Control: 0.1% DMSO. GAPDH, glyceraldehyde-3-phosphate dehydrogenase.

AKT1) were transfected into the MDA-MB-453 cells. In comparison with that in the control cells, the exogenous AKT and phospho-AKT expression significantly increased in MDA-MB-453/myr-AKT1 cells (Fig. 4A, right), and the inhibitory rate was also significantly increased after treatment with DC120 ($p < 0.01$) (Fig. 4B, right). To directly examine cell killing, the sub-G_1 fraction was tested using flow cytometric analysis. The results showed that DC120 decreased cell viability mainly because of the induction of apoptosis, as shown by the increase in sub-G_1 cells. In addition, we observed that the apoptotic cells increased more obviously in CNE2/vector cells compared with that in CNE2/AKT1 shRNA cells and in MDA-MB-453/myr-AKT1 cells compared with that in MDA-MB-453/vector cells, which was consistent with results for the MTT assay. Thus, the data further confirmed that AKT kinase was indeed the target of DC120 treatment in cancer cells.

Effect of DC120 on Phosphorylation of AKT and Its Downstream Targets in Cancer Cells. Because AKT kinase activity is regulated by phosphorylation on two sites, threonine 308 in the activation loop of the catalytic domain and serine 473 in the COOH-terminal regulatory domain, we assessed the effect of DC120 on the phosphorylation status of AKT on Ser473 and Thr308 in cancer cells. The results showed that DC120 up-regulated phosphorylation of Ser473-AKT and Thr308-AKT in a dose- and time-dependent manner, without affecting the amount of AKT (Fig. 5, A and B). It has been stated that AKT exerts its cellular effects through phosphorylation of a number of substrate proteins. More than 20 proteins have been identified as AKT substrates, including the members of the forkhead protein family (FKHR, FKHRL1, and AFX), GSK-3β, endothelial nitric-oxide synthase, mTOR, p21, p27, MDM2, Bad, tuberlin/TSC2, IKKα, and others (Hers et al., 2011; Mannoury la Cour et al., 2011; Wu and Shih, 2011). Because inhibition of substrate phosphorylation can reflect inhibition of AKT activity, we examined whether DC120 could inhibit phosphorylation of downstream targets of AKT. As expected, the phosphorylation levels of FKHR, FKHRL1, GSK-3β, and mTOR were all partially attenuated by DC120 dose de-

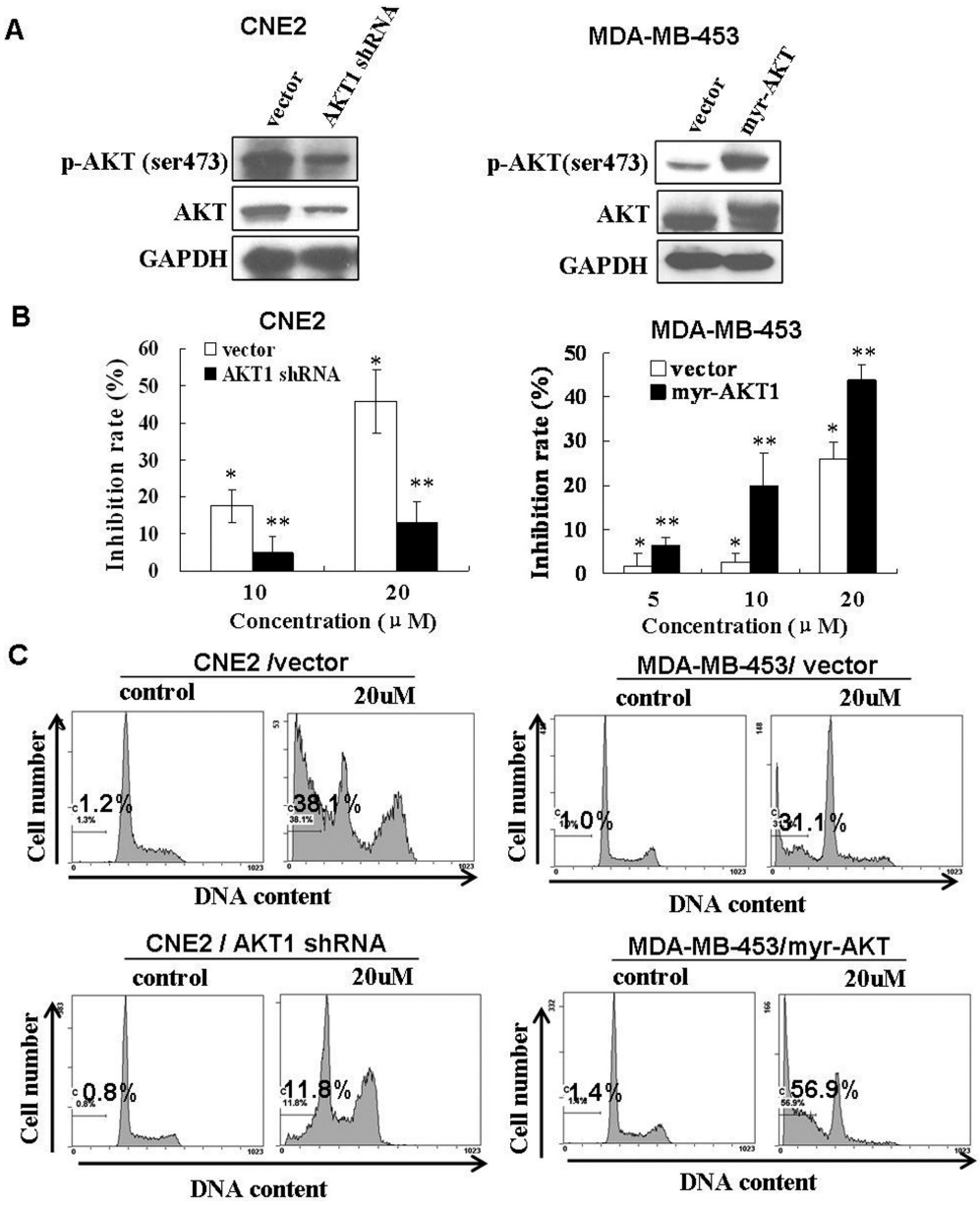

Fig. 4. The cytotoxic effects of DC120 on cancer cells relying on AKT activity. A, the efficiency of AKT1 shRNA stable transfection in CNE2 cells and transient transfection of myr-AKT1 plasmid in MDA-MB-453 cells was analyzed by Western blotting. B, cell viability was determined by MTT assay. CNE2/vector and CNE2/AKT1 shRNA cells were exposed to different concentrations of DC120 for 48 h. MDA-MB-453/vector and MDA-MB-453/myr-AKT1 cells were exposed to different concentrations of DC120 for 24 h. Data are presented as the mean ± S.D. of quadruple determinations (** <0.01 versus *). C, PI fluorescence associated with DNA was measured by flow cytometry. CNE2/vector cells and CNE2/AKT1 shRNA cells were treated with 20 μM DC120 for 48 h. MDA-MB-453/vector cells and MDA-MB-453/myr-AKT cells were treated with 20 μM DC120 for 30 h. The numbers represent the percentages of apoptotic sub-G_1 phase cells. Data represent one of three independent experiments with similar results. GAPDH, glyceraldehyde-3-phosphate dehydrogenase.

pendently and time dependently without affecting the amount of total proteins in CNE2 cells and MDA-453 cells, although the Thr308 and Ser473 phosphorylation of AKT increased concomitantly (Fig. 5, A and B). More precisely, the reduction of phosphorylation of these proteins occurred within 1 h after exposure to 10 μM DC120 in CNE2 and MDA-MB-453 cells.

To further show the correlation between FKHR protein phosphorylation and its cellular localization, CNE2 cells and MDA-MB-453 cells were transiently transfected with pCDNA3-Flag-FKHR plasmids and treated with DC120 for the indicated times. Then we investigated the cellular localization of exogenous FKHR using immunofluorescence staining. We observed that exogenous FKHR protein mainly 1ocated in the cytoplasm without drug treatment but translocated into the nucleus after treatment with DC120 (Fig. 5C). All these data indicated that DC120 could induce cell apoptosis by blocking the AKT downstream signaling pathway including AKT/GSK-3β, AKT/mTOR, and AKT/FOXO in CNE2 cells and MDA-MB-453 cells.

Antitumor Activity of DC120 In Vivo. Because of the potent growth inhibition of DC120 in vitro, its antitumor properties were further examined in vivo. CNE2 xenografts were established and 8% solvent (negative control), DC120, or CTX (positive control) was administered intraperitoneally on day 7 after implantation. No obvious toxicity was observed in mice receiving 8% solvent treatment or 20 mg/kg/day DC120 treatment. Treatment with DC120 at 20 mg/kg/day could obviously suppress the tumor growth and the tumor growth inhibition (T/C percentage) was approximately 38.1% (Fig. 6A). Although the inhibitory rate of the positive control group (100 mg/kg CTX every 5 days) was 84.2%, obvious toxicity was observed, and three mice died during the treatment phase. To determine whether the growth inhibition of DC120 was caused by apoptosis in vivo, frozen tumor sections from CNE2-bearing nude mice were stained with TUNEL to identify the apoptotic cell population. As shown in Fig. 6B, treatment with 8% solvent did not appreciably induce apo-

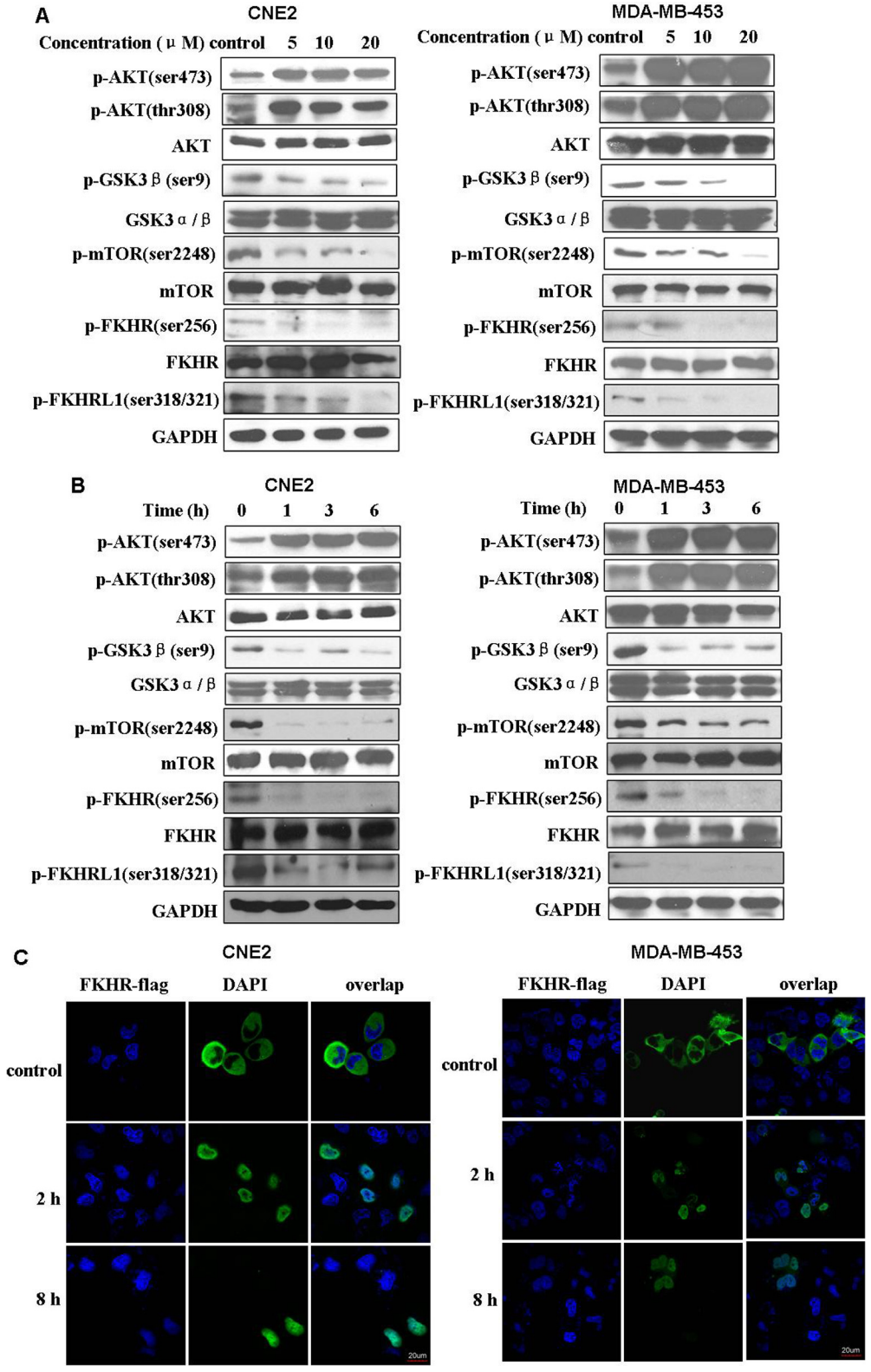

Fig. 5. Effect of DC120 on phosphorylation of AKT and its downstream targets in cancer cells. CNE2 cells or MDA-MB-453 cells were treated with different concentrations of DC120 for 24 h (A) or 10 μM DC120 for different times (B). Total protein isolated was analyzed by immunoblotting with the antibodies indicated. Results are representative of three different experiments. Control: 0.1% DMSO. C, CNE2 cells and MDA-MB-453 cells were transiently transfected with pCDNA3-Flag-FKHR plasmids and were treated with 10 μM DC120 for the indicated times. The cellular localization of exogenous FKHR was examined using immunofluorescence. Original magnification, 100×. GAPDH, glyceraldehyde-3-phosphate dehydrogenase.

ptosis, whereas DC120 at 20 mg/kg/day stimulated a substantially increased number of TUNEL-positive cells in CNE2 tumors, with an obvious increase in the ratio of apoptotic cells. Then we detected the effect of DC120 on the AKT signaling pathway in tumor samples. Immunofluorescence staining in tumor frozen sections showed that the intensity of fluorescence representing the protein level of phospho-GSK3β was +++ in the control group, whereas in the group treated with 20 mg/kg/day DC120, the intensity of fluorescence was + to ++ (Fig. 6C).

U0126 Enhanced DC120-Induced Apoptosis. In this study, we tested the effect of DC120 on the phosphorylation of the MAPK signaling pathway. The results revealed that phospho-JNK, phospho-P38, and phospho-ERK all increased

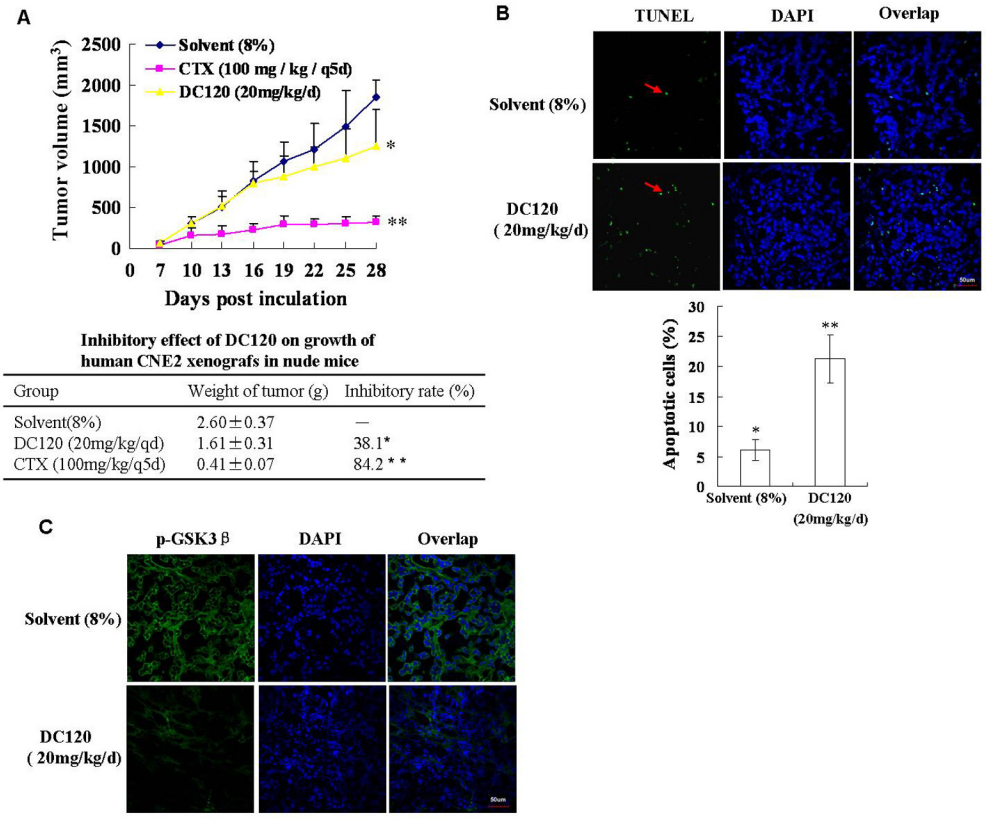

Inhibitory effect of DC120 on growth of human CNE2 xenografs in nude mice

Group	Weight of tumor (g)	Inhibitory rate (%)
Solvent(8%)	2.60±0.37	—
DC120 (20mg/kg/qd)	1.61±0.31	38.1*
CTX (100mg/kg/q5d)	0.41±0.07	84.2 * *

Fig. 6. Effects of DC120 on tumor growth of human CNE2 xenografts in nude mice. A, top, mice bearing established human CNE2 xenografts were given 8% solvent (vehicle group), 20 mg/kg/day DC120, or 100 mg/kg CTX every 7 days (positive group) intraperitoneally for 21 days. Points represent means of tumors ($n = 6$ for vehicle group and DC120 group; $n = 3$ for positive group), and bars represent S.D. Bottom, tumor growth inhibition was calculated. *, $p < 0.05$; **, $p < 0.01$, significantly different from vehicle-treated animals (8% solvent) on day 21 of treatment. B, top, representative images of TUNEL staining of CNE2 xenograft frozen tumor sections after treatment. The apoptotic cells with DNA fragmentation were stained positively as green nuclei (arrows). Bottom, the relative numbers of apoptotic cells were determined by counting TUNEL-positive cells in three random fields (original magnification, 40×) for each sample. Columns represent means, and bars represent S.D. (** <0.01 versus *). C, representative images of immunofluorescence staining of CNE2 xenograft frozen tumor sections for phospho-GSK3β protein. Original magnification, 40×.

obviously after DC120 treatment for 24 h in CNE2 and MDA-MB-453 cells, without affecting the total amount of JNK, P38, and ERK (Fig. 7A), possibly because DC120 induces a feedback loop to activate the MAPK pathway. The activation of feedback loops such as the MAPK pathway by DC120 prompted us to detect the apoptotic effect of the combination of the MEK inhibitor U0126 and DC120 on cancer cells. We noted that treatment with U0126 and DC120 inhibited phospho-ERK expression drastically (Fig. 7B). We also found that the two-drug combination resulted in more apoptotic cells than did treatment with either drug alone. Once combined with U0126, DC120-induced apoptosis increased from 13.9 to 27.5% in CNE2 cells and from 22.1 to 64.1% in MDA-MB-453 cells ($p < 0.01$) (Fig. 7C). These results indicated that U0126 effectively enhanced DC120-induced apoptosis in vitro.

Discussion

Here we report that DC120, a new compound screened out from 2-pyrimidyl-5-amidothiazole ATP-competitive AKT inhibitors, possessed an antiproliferative effect on CNE2 and MDA-MB-453 cells and suppressed CNE2 xenograft tumor growth by inhibiting AKT kinase activity and blocking its signal pathway.

In this study, DC120 showed potent antitumor activity. It not only had a significant inhibitory effect on proliferation of CNE2 and MDA-MB-453 cells in vitro (Fig. 2) but also potently suppressed CNE2 xenograft tumor growth without obvious toxicity at 20 mg/kg/day in vivo (Fig. 6A). Further study confirmed that DC120 decreased cell viability mainly as a result of induction of apoptosis, as demonstrated by increases in sub-G_1 phase cells, annexin V-positive cells, characteristic morphological changes of apoptosis in the nucleus, and cleaved caspase-3 as well as by increases in TUNEL-positive cells in tumor samples (Figs. 3 and Fig. 6B).

In addition, the following data provided validation that DC120 could inhibit AKT kinase activity and block its signal pathway in vitro and in vivo. First, we confirmed that DC120 obviously suppressed AKT kinase activity in a cell-free system by a biochemistry method (Fig. 1B; Supplemental Tables 1 and 2). Second, the cytotoxic effects of DC120 on cancer cells depended on AKT activity (Fig. 4). In MDA-MB-453/myr-AKT1 cells, the AKT signaling pathway is more hyperactivated, rendering the cells highly dependent on this pathway, whereas the opposite situation is seen in CNE2/AKT1 shRNA cells. Because DC120 could inhibit AKT activity, the growth inhibition was much higher in MDA-MB-453/myr-AKT1 cells and much lower in CNE2/AKT1 shRNA cells compared with that in control cells. This result is concurrent with results from another selective AKT inhibitor, triciribine (API-2), which much more potently inhibits cell growth in AKT-overexpressing/activating cells than in those with low levels of AKT (Yang et al., 2004). Third, the ability of AKT to

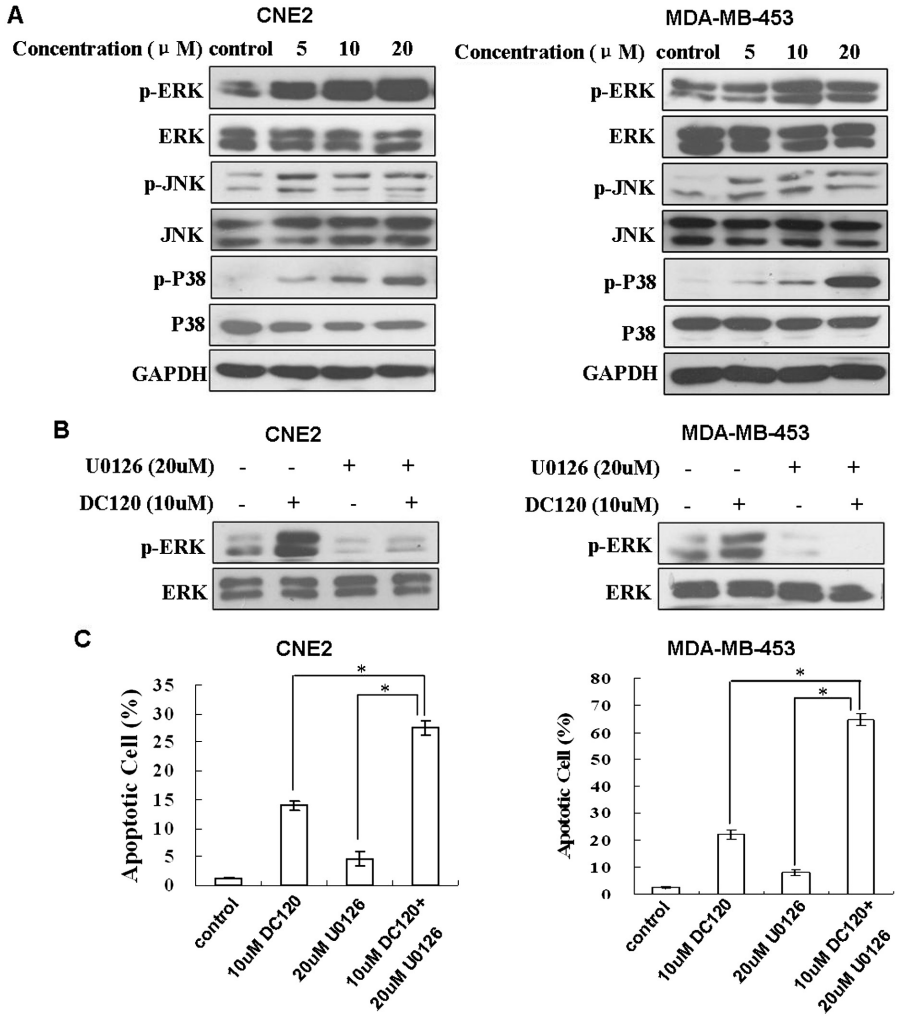

Fig. 7. Treatment with U0126 and DC120 synergistically induced cancer cell apoptosis. A, effect of DC120 on phosphorylation of JNK, ERK, or P38 in cancer cells. CNE2 and MDA-MB-453 cells were treated with different concentrations of DC120 for 24 h. B, effect of the combination of DC120 and U0126 on ERK activation. Cells were treated with DC120, U0126, or the combination at the indicated concentrations for 24 h. C, DC120 and U0126 synergistically induced cancer cell apoptosis. Cells were treated with DC120, U0126, or the combination at the indicated concentrations for 24 h in CNE2 cells or 48 h in MDA-MB-453 cells. Then the annexin V–fluorescein isothiocyanate apoptosis assay was performed. The numbers represent the percentages of annexin V-positive apoptotic cells. Data represent one of three independent experiments with similar results. Columns represent means, and bars represent S.D. *, $p < 0.01$, compared with the single-agent treatments. GAPDH, glyceraldehyde-3-phosphate dehydrogenase.

phosphorylate its downstream targets including FKHR, FKHRL1, GSK-3β, and mTOR was markedly decreased in the presence of the DC120 in vitro and in vivo (Figs. 5, A and B and 6C). We further observed that FKHR translocated into the nucleus upon the reversal of its phosphorylation induced by DC120 in cancer cells (Fig. 5C). Because the reduction in phosphorylation of these downstream effectors occurred early, these effects could not result from induction of apoptosis but instead could conceivably cause apoptosis as a consequence. On the other hand, together with the decrease in phosphorylation of AKT downstream targets, we observed a concomitant increase in the Thr308 and Ser473 phosphorylation of AKT. This increase has been observed with other AKT inhibitors [i.e., (*S*)-1-(1*H*-indol-3-ylmethyl)-2-[5-(3-methyl-1*H*-indazol-5-yl)-pyridin-3-yloxy]-ethylamine (A-443654), 4-[2-(4-amino-1,2,5-oxadiazol-3-yl)-1-ethyl-7-[(3*S*)-3-piperidinylmethoxy]-1*H*-imidazo[4,5-*c*]pyridin-4-yl]-2-methyl-3-butyn-2-ol (GSK690693), and GDC0068)] tested and seems to be a sensitive marker of ATP-competitive AKT inhibition (Luo et al., 2005; Rhodes et al., 2008; Okuzumi et al., 2009). It might be caused by a feedback loop induced by DC120 or might be a direct consequence of DC120 binding to the ATP binding site of AKT (Okuzumi et al., 2009; Chandarlapaty et al., 2011; Chakrabarty et al., 2012). However, as shown by the reduction in the phosphorylation of multiple AKT substrates, DC120 effectively inhibited AKT kinase activity in cells regardless of any feedback hyperphosphorylation of AKT. Taken together, these data suggest that DC120 can inhibit AKT kinase activity and phosphorylate its target effectors, block the AKT signaling pathway, and subsequently initiate apoptotic events.

It is largely believed that combining of AKT inhibitors with other cancer therapeutic agents is a promising way to improve the tumor therapeutic window. It has been recently reported that combination treatment with MK-2206 (an allosteric AKT inhibitor) and selumetinib (AZD6244; a MEK inhibitor) is more effective than treatment with either drug alone in human non–small-cell lung cancer in vitro and in vivo (Meng et al., 2010). In addition, MK-2206 showed synergistic responses in combination with molecular targeted agents such as erlotinib and lapatinib or with cytotoxic agents such as doxorubicin, camptothecin, docetaxel, and carboplatin in lung NCI-H460 or ovarian A2780 tumor cells in vitro and in vivo (Hirai et al., 2010). In the present study, we noted that DC120 induced a feedback loop to activate the MAPK pathway and U0126 effectively enhanced DC120-induced apoptosis in vitro, which indicated that the combination of these two agents has a significant synergistic effect (Fig. 7). In addition, combination of DC120 with other anticancer agents, such as with everolimus (RAD001; a mTOR inhibitor) or radiotherapy is already being tested in our laboratory, and some exciting results have been achieved (data not shown). Exploring the efficacy of the combination of DC120 with other anticancer agents in further studies will be useful to

confirm DC120 as a lead compound targeting AKT signal pathway or for further development.

In summary, our data provide evidence of a sustained antitumor effect and promising development for DC120. DC120 is a potent inhibitor of AKT kinase in tumor cells. Through inhibition of AKT kinase and blockade of its signal pathway, DC120 induces tumor cell apoptosis in vitro and inhibits tumor growth in vivo. These data provide validation for the development of DC120 to treat cancers displaying elevated levels of AKT. Further investigation is required to evaluate whether DC120 is clinically useful in this setting.

Acknowledgments

We gratefully acknowledge Professor William R. Sellers from Department of Adult Oncology and Department of Internal Medicine, Dana-Farber Cancer Institute and Brigham and Women's Hospital, Harvard Medical School for offering pCDNA3- Flag- FKHR plasmid.

Authorship Contributions

Participated in research design: Deng, Ding, and Zhu.
Conducted experiments: Deng, Yang, Chang, Tang, Qin, and Feng.
Contributed new reagents or analytic tools: Chang and Ding.
Performed data analysis: Deng, Yang, Tang, and Zhu.
Wrote or contributed to the writing of the manuscript: Deng, Chang, Ding, and Zhu.

References

Balsara BR, Pei J, Mitsuuchi Y, Page R, Klein-Szanto A, Wang H, Unger M, and Testa JR (2004) Frequent activation of AKT in non-small cell lung carcinomas and preneoplastic bronchial lesions. *Carcinogenesis* **25:**2053–2059.
Bellacosa A, Kumar CC, Di Cristofano A, and Testa JR (2005) Activation of AKT kinases in cancer: implications for therapeutic targeting. *Adv Cancer Res* **94:**29–86.
Caporali S, Levati L, Starace G, Ragone G, Bonmassar E, Alvino E, and D'Atri S (2008) AKT is activated in an ataxia-telangiectasia and Rad3-related-dependent manner in response to temozolomide and confers protection against drug-induced cell growth inhibition. *Mol Pharmacol* **74:**173–183.
Chakrabarty A, Sánchez V, Kuba MG, Rinehart C, and Arteaga CL (2012) Feedback upregulation of HER3 (ErbB3) expression and activity attenuates antitumor effect of PI3K inhibitors. *Proc Natl Acad Sci USA* **109:**2718–2723.
Chandarlapaty S, Sawai A, Scaltriti M, Rodrik-Outmezguine V, Grbovic-Huezo O, Serra V, Majumder PK, Baselga J, and Rosen N (2011) AKT inhibition relieves feedback suppression of receptor tyrosine kinase expression and activity. *Cancer Cell* **19:**58–71.
Chang S, Zhang Z, Zhuang X, Luo J, Cao X, Li H, Tu Z, Lu X, Ren X, and Ding K (2012) New thiazole carboxamides as potent inhibitors of Akt kinases. *Bioorg Med Chem Lett* **22:**1208–1212.
Crowell JA, Steele VE, and Fay JR (2007) Targeting the AKT protein kinase for cancer chemoprevention. *Mol Cancer Ther* **6:**2139–2148.
Deng R, Tang J, Ma JG, Chen SP, Xia LP, Zhou WJ, Li DD, Feng GK, Zeng YX, and Zhu XF (2011) PKB/Akt promotes DSB repair in cancer cells through upregulating Mre11 expression following ionizing radiation. *Oncogene* **30:**944–955.
Deng R, Tang J, Xia LP, Li DD, Zhou WJ, Wang LL, Feng GK, Zeng YX, Gao YH, and Zhu XF (2009) ExcisaninA, a diterpenoid compound purified from Isodon MacrocalyxinD, induces tumor cells apoptosis and suppresses tumor growth through inhibition of PKB/AKT kinase activity and blockade of its signal pathway. *Mol Cancer Ther* **8:**873–882.
Engelman JA (2009) Targeting PI3K signalling in cancer: opportunities, challenges and limitations. *Nat Rev Cancer* **9:**550–562.
Hers I, Vincent EE, and Tavaré JM (2011) Akt signalling in health and disease. *Cell Signal* **23:**1515–1527.
Hirai H, Sootome H, Nakatsuru Y, Miyama K, Taguchi S, Tsujioka K, Ueno Y, Hatch H, Majumder PK, Pan BS, et al. (2010) MK-2206, an allosteric Akt inhibitor, enhances antitumor efficacy by standard chemotherapeutic agents or molecular targeted drugs in vitro and in vivo. *Mol Cancer Ther* **9:**1956–1967.
Institute of Laboratory Animal Resources (1996) *Guide for the Care and Use of Laboratory Animals,* 7th ed, Institute of Laboratory Animal Resources, Commission on Life Sciences, National Research Council, Washington, DC.
Irie HY, Pearline RV, Grueneberg D, Hsia M, Ravichandran P, Kothari N, Natesan S, and Brugge JS (2005) Distinct roles of Akt1 and Akt2 in regulating cell migration and epithelial-mesenchymal transition. *J Cell Biol* **171:**1023–1034.
Janku F, McConkey DJ, Hong DS, and Kurzrock R (2011) Autophagy as a target for anticancer therapy. *Nat Rev Clin Oncol* **8:**528–539.
Kalinsky K, Heguy A, Bhanot UK, Patil S, and Moynahan ME (2011) PIK3CA mutations rarely demonstrate genotypic intratumoral heterogeneity and are selected for in breast cancer progression. *Breast Cancer Res Treat* **129:**635–643.
Lin X, Murray JM, Rico AC, Wang MX, Chu DT, Zhou Y, Del Rosario M, Kaufman S, Ma S, Fang E, et al. (2006) Discovery of 2-pyrimidyl-5-amidothiophenes as potent inhibitors for AKT: synthesis and SAR studies. *Bioorg Med Chem Lett* **16:**4163–4168.
Liu R, Liu D, and Xing M (2012) The Akt inhibitor MK2206 synergizes, but perifosine antagonizes, the $BRAF^{V600E}$ inhibitor PLX4032 and the MEK1/2 inhibitor AZD6244 in the inhibition of thyroid cancer cells. *J Clin Endocrinol Metab* **97:**E173–E182.
LoPiccolo J, Granville CA, Gills JJ, and Dennis PA (2007) Targeting Akt in cancer therapy. *Anticancer Drugs* **18:**861–874.
Luo Y, Shoemaker AR, Liu X, Woods KW, Thomas SA, de Jong R, Han EK, Li T, Stoll VS, Powlas JA, et al. (2005) Potent and selective inhibitors of Akt kinases slow the progress of tumors in vivo. *Mol Cancer Ther* **4:**977–986.
Manning BD and Cantley LC (2007) AKT/PKB signaling: navigating downstream. *Cell* **129:**1261–1274.
Mannoury la Cour C, Salles MJ, Pasteau V, and Millan MJ (2011) Signaling pathways leading to phosphorylation of Akt and GSK-3β by activation of cloned human and rat cerebral D_2 and D_3 receptors. *Mol Pharmacol* **79:**91–105.
Markaryan A, Nelson EG, Tretiakova M, and Hinojosa R (2008) Technical report: immunofluorescence and TUNEL staining of celloidin embedded human temporal bone tissues. *Hear Res* **241:**1–6.
McHardy T, Caldwell JJ, Cheung KM, Hunter LJ, Taylor K, Rowlands M, Ruddle R, Henley A, de Haven Brandon A, Valenti M, et al. (2010) Discovery of 4-amino-1-(7*H*-pyrrolo[2,3-*d*]pyrimidin-4-yl)piperidine-4-carboxamides as selective, orally active inhibitors of protein kinase B (Akt). *J Med Chem* **53:**2239–2249.
Meng J, Dai B, Fang B, Bekele BN, Bornmann WG, Sun D, Peng Z, Herbst RS, Papadimitrakopoulou V, Minna JD, et al. (2010) Combination treatment with MEK and AKT inhibitors is more effective than each drug alone in human non-small cell lung cancer in vitro and in vivo. *PLoS One* **5:**e14124.
Nakanishi T and Ross DD (2012) Breast cancer resistance protein (BCRP/ABCG2): its role in multidrug resistance and regulation of its gene expression. *Chin J Cancer* **31:**73–99.
Okuzumi T, Fiedler D, Zhang C, Gray DC, Aizenstein B, Hoffman R, and Shokat KM (2009) Inhibitor hijacking of Akt activation. *Nat Chem Biol* **5:**484–493.
Rhodes N, Heerding DA, Duckett DR, Eberwein DJ, Knick VB, Lansing TJ, McConnell RT, Gilmer TM, Zhang SY, Robell K, et al. (2008) Characterization of an Akt kinase inhibitor with potent pharmacodynamic and antitumor activity. *Cancer Res* **68:**2366–2374.
Richardson PG, Wolf J, Jakubowiak A, Zonder J, Lonial S, Irwin D, Densmore J, Krishnan A, Raje N, Bar M, et al. (2011) Perifosine plus bortezomib and dexamethasone in patients with relapsed/refractory multiple myeloma previously treated with bortezomib: results of a multicenter phase I/II trial. *J Clin Oncol* **29:**4243–4249.
Seefeld MA, Rouse MB, McNulty KC, Sun L, Wang J, Yamashita DS, Luengo JI, Zhang S, Minthorn EA, Concha NO, et al. (2009) Discovery of 5-pyrrolopyridinyl-2-thiophenecarboxamides as potent AKT kinase inhibitors. *Bioorg Med Chem Lett* **19:**2244–2248.
Sun H, Yu T, and Li J (2011) Co-administration of perifosine with paclitaxel synergistically induces apoptosis in ovarian cancer cells: more than just AKT inhibition. *Cancer Lett* **310:**118–128.
Tokunaga E, Oki E, Egashira A, Sadanaga N, Morita M, Kakeji Y, and Maehara Y (2008) Deregulation of the Akt pathway in human cancer. *Curr Cancer Drug Targets* **8:**27–36.
United Kingdom Co-ordinating Committee on Cancer Research (1998) United Kingdom Co-ordinating Committee on Cancer Research (UKCCCR) Guidelines for the Welfare of Animals in Experimental Neoplasia (second edition). *Br J Cancer* **77:**1–10.
Wei L and Xu Z (2011) Cross-signaling among phosphinositide-3 kinase, mitogen-activated protein kinase and sonic hedgehog pathways exists in esophageal cancer. *Int J Cancer* **129:**275–284.
Whitehall VL, Rickman C, Bond CE, Ramsnes I, Greco SA, Umapathy A, McKeone D, Faleiro RJ, Buttenshaw RL, Worthley DL, et al. (2011) Oncogenic PIK3CA mutations in colorectal cancers and polyps. *Int J Cancer.* http://dx.doi.org/10.1002/ijc.26440.
Wu JB and Shih JC (2011) Valproic acid induces monoamine oxidase A via Akt/forkhead box O1 activation. *Mol Pharmacol* **80:**714–723.
Yang L, Dan HC, Sun M, Liu Q, Sun XM, Feldman RI, Hamilton AD, Polokoff M, Nicosia SV, Herlyn M, et al. (2004) Akt/protein kinase B signaling inhibitor-2, a selective small molecule inhibitor of Akt signaling with antitumor activity in cancer cells overexpressing Akt. *Cancer Res* **64:**4394–4399.
Zhang CH, Wen ZQ, Li JF, Li CZ, Shi M, Yang GW, Lan SM, Zhu Y, Wang F, Zhang YJ, et al. (2008) Inhibition of proliferation and transforming growth factor β3 protein expression by peroxisome proliferators-activated receptor γ ligands in human uterine leiomyoma cells. *Chin Med J* (*Engl*) **121:**166–171.
Zhou WJ, Deng R, Zhang XY, Feng GK, Gu LQ, and Zhu XF (2009) G-quadruplex ligand SYUIQ-5 induces autophagy by telomere damage and TRF2 delocalization in cancer cells. *Mol Cancer Ther* **8:**3203–3213.
Zhu GD, Gandhi VB, Gong J, Thomas S, Woods KW, Song X, Li T, Diebold RB, Luo Y, Liu X, et al. (2007) Syntheses of potent, selective, and orally bioavailable indazole-pyridine series of protein kinase B/Akt inhibitors with reduced hypotension. *J Med Chem* **50:**2990–3003.

Address correspondence to: Professor Xiao-Feng Zhu, State Key Laboratory of Oncology in South China, Cancer Center, Sun Yat-sen University, 651 Dongfeng Road East, Guangzhou 510060, China. E-mail: zhuxfeng@mail.sysu.edu.cn